Oxidation of CaMKII determines cardiotoxic effects of aldosterone

B. Julie He[1,2], **Mei-Ling A. Joiner**[2,8], **Madhu V. Singh**[2,8], **Elizabeth D. Luczak**[2,8], **Paari Dominic Swaminathan**[2,8], **Olha M. Koval**[2], **William Kutschke**[2], **Chantal Allamargot**[5], **Jinying Yang**[2], **Xiaoqun Guan**[2], **Kathy Zimmerman**[4], **Isabella M. Grumbach**[2], **Robert M. Weiss**[2,4], **Douglas R. Spitz**[3], **Curt D. Sigmund**[1,2], **W. Matthijs Blankesteijn**[6], **Stephane Heymans**[7], **Peter J. Mohler**[1,2], and **Mark E. Anderson**[1,2]

[1]Department of Molecular Physiology and Biophysics, The University of Iowa Carver College of Medicine, Iowa City, IA, USA [2]Internal Medicine, The University of Iowa Carver College of Medicine, Iowa City, IA, USA [3]Free Radical and Radiation Biology Program, Department of Radiation Oncology, The University of Iowa Carver College of Medicine, Iowa City, IA, USA [4]Department of Veterans Affairs Medical Center, The University of Iowa Carver College of Medicine, Iowa City, IA, USA [5]Central Microscopy Research Facilities, The University of Iowa Carver College of Medicine, Iowa City, IA, USA [6]Department of Pharmacology and Toxicology, Cardiovascular Research Institute Maastricht, Maastricht University, Maastricht, The Netherlands [7]Center for Heart Failure Research, Cardiovascular Research Institute Maastricht, Maastricht University, Maastricht, The Netherlands

Abstract

Excessive activation of β-adrenergic, angiotensin II, and aldosterone (Aldo) signaling pathways promotes mortality after myocardial infarction (MI), while antagonist drugs targeting these pathways are core therapies for treating post-MI patients. Catecholamines and angiotensin II activate the multifunctional Ca^{2+}/calmodulin-dependent protein kinase II (CaMKII), and CaMKII inhibition prevents isoproterenol- and angiotensin II-mediated cardiomyopathy. Here we show that Aldo exerts direct toxic actions on myocardium by oxidative activation of CaMKII, causing cardiac rupture and increased mortality in mice after MI. Aldo oxidizes CaMKII by recruiting NADPH oxidase, and oxidized CaMKII promotes matrix metalloproteinase 9 (Mmp9) expression in cardiomyocytes. Myocardial CaMKII inhibition, over-expression of methionine sulfoxide reductase A, an enzyme that reduces oxidized CaMKII, or NADPH oxidase inhibition prevented Aldo-enhanced post-MI cardiac rupture. These findings show oxidized myocardial CaMKII

mediates cardiotoxic effects of Aldo on cardiac matrix and establish CaMKII as a nodal signal for the neurohumoral pathways associated with poor outcomes after MI.

Introduction

Ischemic heart disease is a leading cause of death worldwide.[1] Myocardial infarction (MI) is a common presentation of ischemic heart disease. Excessive neurohumoral activity, including sympathetic stimulation and renin-angiotensinaldosterone activation, promotes heart failure and sudden death in patients suffering from MI. Myocardial Ca^{2+}/calmodulin-dependent protein kinase II (CaMKII) is now recognized as a downstream signal that is necessary for the pathological responses to β-adrenergic receptor agonist[2] and angiotensin II[3] stimulation, but the potential intersection between CaMKII and cardiac aldosterone (Aldo) signaling remains unexplored. Circulating Aldo levels increase in patients after MI,[4] and augmented plasma Aldo increases the risk of early mortality after MI.[5] Aldo activates mineralocorticoid receptor (MR) pathways, and MR antagonist drugs significantly reduce mortality in post-MI patients,[6–7] but the cellular pathways activated by Aldo are uncertain. Aldo favors renal sodium reabsorption in the distal convoluted tubule,[8] but recent evidence suggests that Aldo also directly targets myocardium to increase reactive oxygen species (ROS).[9–10] We recently identified a molecular mechanism where CaMKII is activated during MI or angiotensin II infusion by oxidation of paired methionines (Met 281/282) in the CaMKII regulatory domain.[3] The apparent association of Aldo with increased myocardial ROS and premature death suggested the hypothesis that oxidized CaMKII (ox-CaMKII) could play an important, but previously unanticipated, role in pathological responses to Aldo signaling in heart.

We used the mouse MI model supplemented by Aldo infusion (MI + Aldo) to approximate plasma Aldo levels measured in MI patients.[11–12] We found enhanced cardiac rupture in MI + Aldo mice compared to vehicle (MI + Veh) with corresponding increase in CaMKII activity and upregulation of matrix metalloproteinase 9 (*Mmp9*). Our findings identify an unexpected role for CaMKII in the Aldo pathway and highlight an unprecedented capability of myocytes to adversely affect cardiac matrix after MI.

Results

Aldo stimulates CaMKII oxidation and activation

Aldo stimulates cardiac ROS, detected by the ROS fluorescent indicator dihydroethidium (DHE), within 15 minutes in heart tissue from wild-type (WT) mice but to a significantly lesser degree from $Ncf1^{-/-}$ ($p47^{phox-/-}$) mice that lack functional NADPH oxidase[13] ($P = 0.003$, ANOVA, $*P < 0.05$ and $*P < 0.01$, Bonferroni's multiple comparison test versus WT +Veh, Fig. 1a). To determine if Aldo could stimulate CaMKII oxidation, we measured ox-CaMKII in hearts from Aldo- and Veh-infused mice, using an antiserum against oxidized Met 281/282 in the CaMKII autoregulatory domain.[3] We detected increased ox-CaMKII by immunofluorescence (Fig. 1b) and by immunoblotting heart lysates from Aldo- compared to Veh-infused mice ($P = 0.021$, Supplemental Fig. 1a), and confirmed that increased ox-CaMKII affected an increase in Ca^{2+}/calmodulin autonomous CaMKII activity, but without a change in total CaMKII activity ($P = 0.019$, Fig. 1c) in the myocardium of Aldo-compared to Veh-infused mice. We previously showed that angiotensin II infusion can increase CaMKII oxidation.[3,14] To determine if Aldo potentially contributed to the increase in myocardial ox-CaMKII after angiotensin II, we infused mice for six days with angiotensin II in the presence and absence of the mineralocorticoid receptor antagonist spironolactone. We found that hearts from mice infused with angiotensin II and spironolactone had similar CaMKII oxidation compared to mice receiving angiotensin II and

Veh (Supplemental Fig. 1b), suggesting that angiotensin II can increase ox-CaMKII independently of Aldo. Alternatively, increase in Ca^{2+}/calmodulin autonomous CaMKII activity can result from threonine 287 (T287) autophosphorylation. We measured autophosphorylated CaMKII and found that cardiac CaMKII T287 phosphorylation was similar between Veh- and Aldo-infused mice (Supplemental Fig. 1c), consistent with a view that Aldo preferentially increases CaMKII activity by Met 281/282 oxidation.

We used cultured neonatal myocytes to further characterize the mechanism underlying Aldo-induced ROS and CaMKII oxidation. Neonatal myocytes responded to a low concentration of Aldo (10^{-9} mol L^{-1}) with increased ROS, detected by DHE (Supplemental Fig. 2a,b), which is in agreement with the K_d value for MR,[15] suggesting that Aldo-induced ROS is through MR. Furthermore, both ROS and ox-CaMKII were inhibited by the MR antagonist spironolactone (Fig. 1d). These findings supported a concept where Aldo-stimulated ROS production and CaMKII oxidation require MR, and suggested the possibility that some of the clinical benefit of MI patients treated with spironolactone derived from myocardial CaMKII inhibition.

NADPH oxidase is activated by Aldo in endothelial cells,[16] and NADPH oxidase is an effective source of ROS for oxidizing CaMKII in myocardium.[3] Because $Ncf1^{-/-}$ mice show partial protection from Aldo-stimulated cardiac ROS (Fig. 1a), we tested the potential role of NADPH oxidase in Aldo-induced CaMKII oxidation. Pretreatment with the NADPH oxidase inhibitor apocynin prevented Aldo-stimulated ROS and CaMKII oxidation in neonatal myocytes (Fig. 1d). In order to further examine the potential connection between MR and NADPH oxidase, we infected neonatal myocytes with an adenovirus expressing a dominant negative form of the small GTPase Rac1 (N17rac1),[17] because Rac1 is essential for NADPH oxidase activation by MR in endothelial cells.[16] N17rac1 prevented Aldo-induced ROS generation (Fig. 1e), consistent with the hypothesis that MR couples to the NADPH oxidase complex by a Rac1-dependent process in myocardium. Taken together, these findings suggested that Aldo increases myocardial ROS by MR- and Rac1-dependent activation of NADPH oxidase, leading to increased ox-CaMKII.

Myocardial MsrA over-expression lowers ox-CaMKII

Methionine oxidation is a recently discovered mechanism for CaMKII activation, so we sought to better understand the regulation of this dynamic process. Hearts from mice lacking MsrA in all tissues show increased susceptibility to CaMKII oxidation by angiotensin II and increased mortality after MI.[3] In order to test if myocardial MsrA supplementation could reduce the level of ox-CaMKII after Aldo, we infected neonatal myocytes with adenovirus expressing human MsrA. MsrA over-expression reversed Aldo-stimulated CaMKII oxidation (Fig. 2a), suggesting that endogenous levels of MsrA in WT myocytes were insufficient for maximal methionine reductase activity against oxidized CaMKII.

We next developed a mouse model of myocardial restricted MsrA over-expression to determine if CaMKII oxidation is critical to Aldo-induced pathology *in vivo*. MsrA transgenic mice have greater MsrA protein expression (Fig. 2b) and reductase activity (Fig. 2c) compared to WT littermates. MsrA transgenic mice had similar baseline left ventricular ejection fractions compared to WT littermates (Supplemental Fig. 3). However, ox-CaMKII was considerably diminished in hearts from MsrA transgenic mice compared to WT littermates in response to Aldo (Fig. 2d). In contrast, unlike the $Ncf1^{-/-}$ mice, MsrA over-expression had no effect on total Aldo-induced ROS production (Fig. 2e), as detected by DHE fluorescence, suggesting that MsrA over-expression results in a highly targeted anti-oxidant effect.

MI and Aldo promote cardiac rupture

Our data so far suggested that Aldo increased oxidized and activated CaMKII in myocytes *in vivo* and *in vitro*. We next asked how CaMKII activation could contribute to cardiotoxic effects of Aldo after MI. Aldo antagonist drugs are proven to reduce mortality associated with MI.[6–7] In patients with acute MI, the plasma Aldo concentration increases stepwise with the risk of mortality.[5] Plasma Aldo levels are elevated over a wide range after MI, up to 20-fold excess over baseline,[18] and may reach as high as 10^{-7} mol L^{-1}.[12] We measured plasma Aldo in mice after MI, but found only a modest (approximately two-fold) increase, suggesting that robust elevation in circulating Aldo post-MI is not characteristic of mice. In order to `humanize' our mouse model to better reflect the experience of patients with elevated plasma Aldo after MI, we infused Aldo to reach seven-fold over baseline (Low dose), similar to what is commonly observed in heart failure patients.[19] In addition, to mimic what is seen in very high risk patients with severely elevated Aldo after MI,[11–12] we infused Aldo to approximate the 20-fold increase in circulating Aldo level over baseline (High dose) (Supplemental Fig. 4). WT MI + Aldo mice had significantly reduced survival at the high Aldo dose and showed a trend towards reduced survival at the low Aldo dose (34.5% High dose versus 69.0% Veh, $P = 0.007$, and 42.9% Low dose versus 69.0% Veh, $P = 0.083$, Fig. 3a) compared to WT MI + Veh mice within the first five days after surgery. Surprisingly, excess mortality in the MI + Aldo group was due to cardiac rupture (Fig. 3b and c). Since MI + Aldo at the High dose gave the most prominent rupture and mortality phenotype, we used this dose in all subsequent studies.

When we investigated CaMKII oxidation in the cardiac lysates obtained two weeks after MI or sham surgery, we found significantly increased ox-CaMKII ($P = 0.039$, Fig. 3d). Ca^{2+}/ calmodulin autonomous CaMKII activity ($P < 0.001$, Fig. 3e) was elevated in cardiac lysates at 1 week after MI + Aldo compared to MI + Veh. Thus, MI + Aldo increases cardiac ox-CaMKII, autonomous CaMKII activity, and cardiac rupture. Aldo can increase blood pressure and contribute to heart failure after MI by increasing renal sodium reabsorption and intravascular volume. We investigated blood pressure in WT mice infused with Aldo for two weeks but found no significant blood pressure differences, compared to Veh-infused mice (Supplemental Fig. 5a–c), likely because our model did not include increased dietary sodium. To test this hypothesis, we repeated Aldo infusion in the presence of 1% NaCl and 0.75% KCl supplemented to drinking water and found a significant increase in systolic blood pressure ($P = 0.020$, Supplemental Fig. 5d–f). Likewise, MI itself does not significantly increase blood pressure (Supplemental Fig. 5g–i). Echocardiographic measurements, performed at 3 to 6 days following surgery, the time period when rupture predominantly occurs, suggested equivalent myocardial function between MI + Aldo and MI + Veh mice and were also statistically similar between mice succumbing to cardiac rupture and mice resisting rupture (Supplemental Fig. 6). In fact, mice with rupture trend towards a decreased ejection fraction compared to mice with no rupture ($P = 0.189$, Supplemental Fig. 6r), suggesting that increased contractile force is unlikely to underlie the increased propensity toward cardiac rupture in this model. Collectively, these measurements suggested that excessive death due to cardiac rupture in the MI + Aldo mice correlated with increased ox-CaMKII and CaMKII activity, but was independent of effects on blood pressure and myocardial contraction.

CaMKII inhibition protects against cardiac rupture

Myocardial CaMKII inhibition is known to reduce adverse left ventricular remodeling three weeks after MI.[2–3] However, to our knowledge, the potential for myocardial CaMKII to affect mortality after MI is untested. Based on elevated CaMKII activity in the MI + Aldo model, we hypothesized that CaMKII inhibition may improve survival. Indeed, we observed a significant survival advantage in AC3-I mice over WT mice in the first week after MI ($P =$

0.007, Fig. 3f). We repeated MI + Aldo studies in AC3-I mice and found a trend towards protection from post-MI mortality despite Aldo supplementation (73.7% survival for AC3-I versus 33.3% for WT littermates, P = 0.075, Fig. 3g). AC3-I mice showed reduced cardiac rupture, similar to AC3-I MI + Veh mice, suggesting that myocardial CaMKII activity was required for increased mortality and cardiac rupture in our MI + Aldo model (Fig. 3h). Taken together, our findings show that the acute effects of Aldo to promote cardiac rupture after MI required myocardial CaMKII activity.

To determine the role of ox-CaMKII in survival following MI + Aldo, we repeated MI studies in $Ncf1^{-/-}$, $MsrA^{-/-}$, and our newly developed MsrA transgenic mice. $Ncf1^{-/-}$ mice were protected from MI + Aldo-induced cardiac rupture (0/11), supporting the importance of ROS in cardiac rupture after MI. $MsrA^{-/-}$ mice show enhanced myocardial apoptosis, maladaptive left ventricular remodeling, and increased mortality after MI.[3] We found a pronounced susceptibility to rupture in $MsrA^{-/-}$ MI + Aldo mice (7/10), whereas MsrA transgenic mice had a survival advantage (P = 0.048, Fig. 3i) and were protected from MI + Aldo-induced cardiac rupture compared to WT littermates (P = 0.047, Fig. 3j). These studies showed that conditions favoring suppression of myocardial ox-CaMKII dramatically improved survival by reducing cardiac rupture in the first week after MI. Overall, these findings support a model where MI and Aldo increase CaMKII oxidation, leading to cardiac rupture and premature death.

MI- and Aldo-induced Mmp9 require CaMKII

We next focused on the gelatinases, Mmp2 and Mmp9, known mediators of the rupture phenotype in mice.[20–21] We used a gene array comparing mRNA isolated from AC3-I and control hearts after MI[22] to identify candidate CaMKII-regulated genes that could contribute to ventricular rupture. We confirmed these gene array data using qRT-PCR and found *Mmp9* expression was increased by MI in control mice but to a significantly lesser degree in AC3-I mice with myocardial-delimited CaMKII inhibition (Fig. 4a). Neutrophils and macrophages are the predominant sources of post-MI Mmp9 release.[21,23] However, since the AC3-I model is a cardiomyocyte specific model of CaMKII inhibition, we first investigated myocyte-derived Mmp9 by immunofluorescence and z-stack analysis of images acquired by confocal microscopy. We isolated ventricular myocytes from the infarct region and, surprisingly, found that MI + Aldo significantly increased Mmp9 in cardiomyocytes over sham operated controls and that myocytes from AC3-I positive mice have reduced Mmp9 staining compared to WT (Fig. 4b). Z-stack analysis further showed that Mmp9 expression is cytoplasmic and appears perpendicular to α-actinin staining (Fig. 4b Inset). These findings suggested a model of MI-provoked cardiac rupture, corresponding to a myocardial CaMKII-dependent increase in Mmp9 expression. We repeated the immunofluorescence and z-stack analyses on human heart samples obtained from individuals who died of MI alone or MI complicated by rupture. We found an increase in punctuate intracellular staining of Mmp9 within cardiomyocytes located in the infarct region compared to the remote region from samples with MI and rupture (Fig. 4c). In contrast, no Mmp9 increase was detected in the infarct region of MI samples obtained from hearts of subjects who died without cardiac rupture (Fig. 4c). Thus, our findings reveal a parallel increase in cardiomyocyte-derived Mmp9 that correlates with a rupture phenotype in both mice and humans.

Our data in cardiomyocytes suggested that the contribution of myocardial Mmp9 is important for post-MI cardiac rupture in MI + Aldo mice. However, invading cells that respond to MI are likely the major source of Mmp9,[21,23] so we next assayed for potential effects of myocardial CaMKII inhibition on the cellular response to MI. We measured myeloperoxidase (MPO), a marker of neutrophil content,[24] and found that both MPO immunohistochemical staining (Fig. 5a) and MPO activity (Fig. 5b) increase after MI, but remain similar between WT and AC3-I mice 24 hours after MI + Aldo. The number of MPO

positive cells is also similar between samples from ruptured and non-ruptured WT MI + Aldo mice (Fig. 5a). We then stained for Mac-3 in samples 3 days after MI + Aldo to identify macrophages, which comprise the pool of cells in the delayed inflammatory influx that infiltrate after neutrophils.[21] We found no difference in cumulative Mac-3 staining between WT and AC3-I mice (Fig. 5c). We next asked if the protection from cardiac rupture in AC3-I hearts could derive from reduced Mmp9 expression in infiltrating inflammatory cells in AC3-I compared to WT hearts after MI + Aldo. We performed double immunostaining for the neutrophil membrane marker NIMP-R14[25] and Mmp9 and for Mac-3 and Mmp9 in hearts from WT and AC3-I MI + Aldo mice. We found no significant differences in Mmp9 expression in NIMP-R14 or Mac-3 positive cells between WT and AC3-I mice ($P = 0.787$ and $P = 0.329$, Supplemental Fig. 7), suggesting that inflammatory cells in WT and AC3-I mice produce similar levels of Mmp9. We next assessed post-MI cardiac fibrosis by examining profibrotic genes known to be activated in cardiomyocytes by a myocyte enhancer factor transcriptional pathway.[26] We found that *Col1a2* and *Col3a1* mRNA expression were increased after MI + Aldo in WT mice, but reduced in AC3-I mice (Fig. 5d). In contrast, *Ctgf* mRNA expression increased equally in WT and AC3-I mice after MI + Aldo. However, determination of the total collagen deposition by Masson's trichrome staining revealed similar increases in collagen after MI + Aldo in WT and AC3-I mice (Fig. 5e). We interpret these data to show that myocardial AC3-I expression suppressed myocardial expression of Mmp9, but without affecting total fibrosis compared to WT MI + Aldo mice.

Aldo regulates Mmp9 promoter activity

We next challenged neonatal myocytes with Aldo and found a significant increase in Mmp9 activity by gelatin zymography, whereas MMP2 activity, also detectable by this method, was not significantly changed (Fig. 6a). We validated *Mmp9* as a transcriptionally regulated target in neonatal myocytes (Fig. 6b), an effect attenuated in the presence of the mineralocorticoid receptor antagonist spironolactone (Supplemental Fig. 2c). CaMKII activity was critical for Aldo stimulated *Mmp9* expression, because myocytes with reduced CaMKII expression due to pretreatment with shRNA targeting the major myocardial CaMKII isoform (CaMKIIδ) were ineffective in expressing *Mmp9* in response to Aldo (Fig. 6b). Adenoviral over-expression of CaMKII in neonatal myocytes was sufficient to drive an increase in *Mmp9* expression (Fig. 6c). Since $Mmp9^{-/-}$ mice are known to resist MI-induced cardiac rupture,[21] we subjected $Mmp9^{-/-}$ mice to MI + Aldo treatment and observed a trend towards protection from rupture (1/8 versus 8/13 in control C57BL/6, $P = 0.067$), supporting the concept that Mmp9 is important for increased cardiac rupture in MI + Aldo mice.

Prior work in astrocytes demonstrated CaMKII induction of *Mmp9* promoter activity through JNK and c-jun activation and subsequent recruitment of the transcription factor AP-1.[27] However, when we tested for JNK and c-jun phosphorylation in cardiac lysates, we found no statistical difference between Aldo and Veh infusion (Supplemental Fig. 8), suggesting that AP-1 recruitment is a minor component of the transcription signaling activated by Aldo in our model. We next analyzed the murine *Mmp9* gene promoter for potential CaMKII responsive regulatory sequences and identified an A/T-rich element similar to other validated binding sites for myocyte enhancer factor 2 (MEF2), located approximately 670bp upstream of the murine *Mmp9* transcription start site[28] (Fig. 6d). CaMKII is a known upstream activator of MEF2 through phosphorylation-dependent derepression of transcription by type II histone deacytelases.[29] We focused on this candidate MEF2 binding site because Aldo infusion significantly ($P = 0.002$) increased MEF2 driven β-galactosidase activity in MEF2-lacZ reporter mice[30] over Veh-infused controls (Fig. 6e). Aldo-induced MEF2 activation was eliminated by interbreeding MEF2 reporter mice into a background of myocardial CaMKII inhibition due to AC3-I expression (MEF2xI/Aldo) (Fig.

6e). To determine if the putative MEF2 binding site was functional, we constructed an *Mmp9* promoter-luciferase reporter and a corresponding mutant control reporter with point mutations in the candidate MEF2 binding site (Fig. 6d). Aldo treatment significantly increased *Mmp9* promoter driven luciferase activity in neonatal myocytes, but Aldo had no effect on the mutant control reporter (Fig. 6f). Our findings identified *Mmp9* as a novel target of MI + Aldo/CaMKII/MEF2 regulated transcription in myocytes, distinct from traditional gene targets involved in muscle differentiation, development, and hypertrophy (Fig. 6g).[30–31]

Discussion

Our study provides new evidence supporting an important and under-recognized role for myocardial CaMKII in cardiac matrix biology. We show that MI + Aldo activates CaMKII to produce mortality by cardiac rupture with concurrent upregulation of Mmp9. Mmp9 is known to increase post-MI cardiac rupture, but it was presumed that the source of Mmp9 was exclusively related to extra-myocardial cells.[21] The present results do not refute the production of extra-myocardial Mmp9 in post-MI remodeling nor exclude the involvement of other proteolytic enzymes likely upregulated in this model, but rather reveal that inhibition of CaMKII in myocardial cells *in vitro* and *in vivo* was sufficient to reduce Mmp9 and cardiac rupture, suggesting that cardiomyocytes and cardiac-delimited CaMKII contributes to a critical threshold of Mmp9 activity in the post-MI heart. These results add to other recent findings showing that myocardium is an active participant in pro-inflammatory signaling after MI by CaMKII-dependent activation of NF-κB mediated transcription,[22] and highlight the surprising connections between ROS, CaMKII, myocardium, and matrix in cardiac disease. Chang et al found that MEF2-induced *Mmp10* transcription is detrimental for vasculogenesis,[32] suggesting that our findings may have far-reaching implications for other processes, such as cancer metastasis,[33] atherosclerosis,[34] and stroke,[35] where elevated ROS and hyperactive matrix remodeling play important roles in disease progression.

Although the role of an ox-CaMKII pathway to promote myocardial Mmp9 expression remains unproven in humans, we observed a parallel increase in Mmp9 expression in mouse and human heart samples after MI and cardiac rupture, indicating that myocardial Mmp9 is a marker for rupture in humans who suffer MI. While we did not find differences in the overall level of infiltrating neutrophils or macrophages nor in Mmp9 expression by these cells, our findings do not exclude the possibility that other functional differences in the infiltrating inflammatory cells between WT and AC3-I transgenic mice may contribute to the protective effects of myocardial CaMKII inhibition. Short-term metalloproteinase inhibition was previously shown to protect against cardiac rupture, but long-term inhibition led to cardiac dysfunction and premature death due to defective neovasculogenesis.[21] These results, combined with previous work from our group and others on the cardioprotective benefits of CaMKII inhibition in structural heart disease,[2,14,36–37] suggest that CaMKII inhibition is a viable alternative to global metalloproteinase inhibition for preventing or reducing the incidence of post-MI cardiac rupture and death.

Excessive oxidation is a fundamental feature of major cardiovascular diseases and is linked to a wide array of processes associated with maladaptive responses to MI, including myocardial hypertrophy,[38–39] apoptosis,[3] interstitial fibrosis,[38–39] increased matrix metalloproteinase activity,[39] inflammation,[22] and left ventricular cavity dilation.[3,38] However, broad spectrum anti-oxidant supplements have not proven beneficial in clinical trials,[40–42] while new but preliminary studies with anti-oxidants engineered for local action[43] and molecular specificity[44] appear to show benefit. The failure of broad spectrum anti-oxidant supplements coupled with the preliminary success of molecularly and subcellularly targeted anti-oxidants suggest improved understanding of ROS-responsive

disease pathways will be necessary to identify and develop useful new treatments that interrupt pathological oxidation processes locally, in specific signaling pathways most relevant to progression of cardiovascular disease.[45] Human myocardium after MI shows elevated NADPH oxidase activity,[46] while hearts from $Ncf1^{-/-}$ mice lacking functional NADPH oxidase are protected from increases in ROS, adverse left ventricular remodeling and death after MI surgery.[38] Our findings provide new insights into pathological mechanisms of ROS after MI, by showing that enhanced activation of MsrA in myocardium, by transgenic over-expression, protected against cardiac rupture in MI + Aldo mice by reducing ox-CaMKII. Our study suggests a potential new paradigm for molecularly targeted anti-oxidant therapy by modulating CaMKII oxidation and hyperactivity after MI.

Neurohumoral pathways initiated by β-adrenergic receptor agonists[47], angiotensin II[48], and Aldo[6–7] are major therapeutically validated targets for reducing mortality and heart failure after MI. CaMKII is now recognized to be a downstream signal activated by the β-adrenergic[2] and angiotensin II[3] pathways in myocardium, and CaMKII inhibition prevents or attenuates MI-, isoproterenol-, and angiotensin II- induced myocardial hypertrophy, apoptosis and dysfunction.[2–3,49] Here we show that CaMKII is also activated in myocytes by Aldo through a non-G-protein receptor coupled, MR pathway and that CaMKII is required for early pathological effects of Aldo after MI when both CaMKII and ROS become elevated. Taken together with earlier results,[2–3] our new findings identify CaMKII as a `master' signaling node for the neurohumoral pathways targeted by frontline drugs used to treat post-MI patients.

Cardiac rupture occurs as an early consequence of MI and is a particularly challenging clinical problem, because it occurs with minimal warning and progresses rapidly to death in the majority of cases, despite surgical intervention.[50] Development of preventative therapy is limited by a lack of molecular understanding of the signaling pathways underlying cardiac rupture. The reported incidence of cardiac rupture among MI associated in-hospital deaths can be as high as 15%,[50] a value similar to what we observed in MI + Veh studies in WT mice. Rupture is the second major cause of cardiac sudden death within the first month after MI.[51] Current recommendations support initiation of β-adrenergic receptor and angiotensin II antagonist drugs immediately upon diagnosis of MI,[52–53] and our study provides a novel mechanism and rationale for a recently initiated clinical translational study of rapid initiation of MR antagonist or CaMKII inhibitor drugs to reduce the incidence of post-MI mortality,[54] including mortality due to ventricular rupture.

Online Methods

Mouse Models

The $Ncf1^{-/-}$ ($p47^{phox-/-}$) and $Mmp9^{-/-}$ mice were purchased from The Jackson Laboratory. The $MsrA^{-/-}$ mice[3] and MEF2-lacZ reporter mice[30] were previously described. We constructed AC3-I transgenic mice with myocardial CaMKII inhibition, as previously reported.[2] We interbred AC3-I positive mice with MEF2-lacZ reporter mice for at least five generations. To generate the MsrA transgene, human MsrA cDNA was subcloned into pBS-αMHC vector backbone with flanking MluI and BspeI restriction sites. The transgene was excised, purified and microinjected into pronuclei of B6SJL mice (C57BL/6J × SJL/J). ICR blastocysts were microinjected with the ES cells. Transgenic mice were maintained by backcross breeding to C57BL/6J for at least four generations. All mice were fed standard mouse chow (7013, Teklad Premier Laboratory Diets) and water ad libitum. We performed studies on 8–20-week-old male mice. We confirmed genotypes by PCR. All animal procedures met the guidelines set forth by the Institutional Animal Care and Use Committee at the University of Iowa.

Myocardial Infarction and Echocardiography

Mice underwent myocardial infarction and simultaneous implantation of Aldo (High dose 1.44 mg kg^{-1} d^{-1} or Low dose 0.12 mg kg^{-1} d^{-1}) or Veh (5% ethanol in normal saline) containing osmotic minipumps (Model 2002, Alzet) as previously described.[3] Cardiac rupture was identified by blood clotting in the chest cavity and ventricular wall tear. We recorded baseline and post-operative transthoracic echocardiograms in conscious mice as previously described.[55] Images were acquired and analyzed by an operator blinded to mouse genotype and treatment.

Cell Culture and Viral Constructs

We isolated adult ventricular myocytes as previously described[56] with minor modifications. Briefly, after Langendorff perfusion, hearts were transferred to a dissecting microscope. We identified the infarct region by the blanched appearance of a thinned area in the ventricular free wall. The 1–2 mm borderzone between this and normal appearing myocardium was excised and minced. Neonatal mouse ventricular myocytes were isolated according to previously published methods[57] with minor modifications. We stimulated cells with Aldo (100 nmol L^{-1}) or Veh (phosphate buffered saline) in the presence or absence of spironolactone (10 μmol L^{-1}) or apocynin (100 μmol L^{-1}), as indicated. Human MsrA cDNA was subcloned into pAd5-CMV-IRES-eGFP via blunt ligation. Adenovirus was generated at the University of Iowa Gene Transfer Vector Core facility. The Rac1 dominant negative (N17rac1) construct,[17] the CaMKII shRNA and rescue constructs,[3] and the adenoviral CaMKII construct[58] were described elsewhere.

qRT-PCR

We isolated total RNA from ventricles using TRIzol reagent (Invitrogen) and from neonatal myocytes using RNeasy Plus Mini (QIAGEN) according to manufacturers' instructions. q-PCR for *Mmp9* was performed with Sybr Green detection on IQ® Cycler (Bio-Rad) using the following primers—*Mmp9* sense 5'–GAAGGCAAACCCTGTGTGTT–3' and antisense 5'–AGAGTACTGCTTGCCCAGGA–3' and *Gapdh* sense 5'–CATTTCCTGGTATGACAATGAATACG–3' and antisense 5'–TCCAGGGTTTCTTACTCCTTGGA–3'. We quantified mRNA levels with the delta delta Ct method. Specificity was determined with melt curve analysis. Additional q-PCR was performed with the following Taqman probes from ABI: *Ctgf*, Mm00515790_g1, *Col3a1*, Mm00802331_m1, *Col1a2*, Mm00483888_m1, and *Gapdh* Mm99999915_g1.

Gelatin Zymography

Tissue culture supernatant from treated primary cells was incubated with gelatin-sepharose (Amersham) in the presence of 1,10-phenanthroline (5 mmol L^{-1}) to inhibit metalloproteinase activity. Following binding and washing, protein was released with sample loading buffer. Samples were electrophoresed on Novex® 10% zymogram gels co-polymerized with gelatin (Invitrogen). The SDS in the gel was exchanged with Triton in the washing buffer. The gel was allowed to develop overnight. Proteolytic activity was visualized as white bands on a background of Coomassie Brilliant Blue stain.

MsrA Activity

We determined relative reductase activity in whole heart homogenates indirectly by spectrophotometric monitoring of the decline in NADPH, consumed in the thioredoxin and thioredoxin reductase system during the recycling of MsrA.[59]

Myeloperoxidase (MPO) Activity

We extracted MPO from whole heart with hexadecyltrimethylammonium bromide-based lysis and assayed according to previously published methods[24]. Briefly, the reaction of hydrogen peroxide and o-dianisidine dihydrochloride (reduced, colorless) was catalyzed by the addition of MPO in heart lysates to yield a yellow-orange end product read spectrophotometrically at 460 nm. All readings were normalized to total protein.

Luciferase Reporter Assay

The mineralocorticoid and glucocorticoid responsive hormone response element firefly luciferase reporter was purchased (Clontech). The murine *Mmp9* promoter (−1261 to +1) was subcloned into pTAL-luc (Clontech) via blunt end ligation. The mutant *Mmp9* promoter luciferase construct was obtained with QuikChange Site Directed Mutagenesis (Stratagene). Transfection of a firefly luciferase reporter plus pRL-TK (Promega) was achieved with Fugene 6 (Roche). We performed luciferase assays with the Dual Luciferase Reporter kit (Promega). Fluorescence was quantified on a microplate fluorometer.

Immunoblot and Immunofluorescence

We performed immunoblotting and immunofluorescence as previously described[3] with minor modifications. DHE staining with light fixation was adapted from a published method,[60] then followed by immunofluorescence. Image processing for relative intensity was performed on Image J. Staining and quantification were performed by investigators and technical personnel blinded to the treatments.

Statistics

Survival analysis was performed with the Log rank test. Contingency analysis was analyzed with the Yate's corrected chi-square test. All other statistical significance was evaluated with Student's t-test or one-way ANOVA, as appropriate. Bonferroni's correction was applied for multiple comparisons. All values were expressed as means ± s.e.m. $P < 0.05$ was considered significant.

Additional methods

Additional methodology is described in Supplemental Methods.

Supplementary Material

Refer to Web version on PubMed Central for supplementary material.

Acknowledgments

References

1. Lopez AD, Mathers CD, Ezzati M, Jamison DT, Murray CJ. Global and regional burden of disease and risk factors, 2001: systematic analysis of population health data. Lancet. 2006; 367:1747–1757. [PubMed: 16731270]

2. Zhang R, et al. Calmodulin kinase II inhibition protects against structural heart disease. Nature medicine. 2005; 11:409–417.

3. Erickson JR, et al. A dynamic pathway for calcium-independent activation of CaMKII by methionine oxidation. Cell. 2008; 133:462–474. [PubMed: 18455987]

4. Gutierrez-Marcos FM, et al. Atrial natriuretic peptide in patients with acute myocardial infarction without functional heart failure. Eur Heart J. 1991; 12:503–507. [PubMed: 1829681]

5. Beygui F, et al. High plasma aldosterone levels on admission are associated with death in patients presenting with acute ST-elevation myocardial infarction. Circulation. 2006; 114:2604–2610. [PubMed: 17116769]

6. Pitt B, et al. Eplerenone, a selective aldosterone blocker, in patients with left ventricular dysfunction after myocardial infarction. The New England journal of medicine. 2003; 348:1309–1321. [PubMed: 12668699]

7. Pitt B, et al. The effect of spironolactone on morbidity and mortality in patients with severe heart failure. Randomized Aldactone Evaluation Study Investigators. N Engl J Med. 1999; 341:709–717. [PubMed: 10471456]

8. Reilly RF, Ellison DH. Mammalian distal tubule: physiology, pathophysiology, and molecular anatomy. Physiol Rev. 2000; 80:277–313. [PubMed: 10617770]

9. Rude MK, et al. Aldosterone stimulates matrix metalloproteinases and reactive oxygen species in adult rat ventricular cardiomyocytes. Hypertension. 2005; 46:555–561. [PubMed: 16043662]

10. Johar S, Cave AC, Narayanapanicker A, Grieve DJ, Shah AM. Aldosterone mediates angiotensin II-induced interstitial cardiac fibrosis via a Nox2-containing NADPH oxidase. FASEB J. 2006; 20:1546–1548. [PubMed: 16720735]

11. Nakamura S, et al. Possible association of heart failure status with synthetic balance between aldosterone and dehydroepiandrosterone in human heart. Circulation. 2004; 110:1787–1793. [PubMed: 15364798]

12. Rousseau MF, et al. Beneficial neurohormonal profile of spironolactone in severe congestive heart failure: results from the RALES neurohormonal substudy. J Am Coll Cardiol. 2002; 40:1596–1601. [PubMed: 12427411]

13. Huang CK, Zhan L, Hannigan MO, Ai Y, Leto TL. P47(phox)-deficient NADPH oxidase defect in neutrophils of diabetic mouse strains, C57BL/6J-m db/db and db/+ J Leukoc Biol. 2000; 67:210–215. [PubMed: 10670582]

14. Swaminathan PD, et al. Oxidized CaMKII causes cardiac sinus node dysfunction in mice. J Clin Invest. 2011; 121:3277–3288. [PubMed: 21785215]

15. Kusch M, Farman N, Edelman IS. Binding of aldosterone to cytoplasmic and nuclear receptors of the urinary bladder epithelium of Bufo marinus. Am J Physiol. 1978; 235:C82–89. [PubMed: 211852]

16. Iwashima F, et al. Aldosterone induces superoxide generation via Rac1 activation in endothelial cells. Endocrinology. 2008; 149:1009–1014. [PubMed: 18079208]

17. Zimmerman MC, et al. Requirement for Rac1-dependent NADPH oxidase in the cardiovascular and dipsogenic actions of angiotensin II in the brain. Circ Res. 2004; 95:532–539. [PubMed: 15271858]

18. Weber KT. Aldosterone in congestive heart failure. The New England journal of medicine. 2001; 345:1689–1697. [PubMed: 11759649]

19. Swedberg K, Eneroth P, Kjekshus J, Wilhelmsen L. Hormones regulating cardiovascular function in patients with severe congestive heart failure and their relation to mortality. CONSENSUS Trial Study Group. Circulation. 1990; 82:1730–1736. [PubMed: 2225374]

20. Matsumura S, et al. Targeted deletion or pharmacological inhibition of MMP-2 prevents cardiac rupture after myocardial infarction in mice. J Clin Invest. 2005; 115:599–609. [PubMed: 15711638]

21. Heymans, et al. Inhibition of plasminogen activators or matrix metalloproteinases prevents cardiac rupture but impairs therapeutic angiogenesis and causes cardiac failure. Nature medicine. 1999; 5:1135.

22. Singh MV, et al. Ca2+/calmodulin-dependent kinase II triggers cell membrane injury by inducing complement factor B gene expression in the mouse heart. J Clin Invest. 2009; 119:986–996. [PubMed: 19273909]

23. van den Borne SW, et al. Increased matrix metalloproteinase-8 and -9 activity in patients with infarct rupture after myocardial infarction. Cardiovasc Pathol. 2009; 18:37–43. [PubMed: 18402833]

24. Bradley PP, Priebat DA, Christensen RD, Rothstein G. Measurement of cutaneous inflammation: estimation of neutrophil content with an enzyme marker. J Invest Dermatol. 1982; 78:206–209. [PubMed: 6276474]

25. Nahrendorf M, et al. Activatable magnetic resonance imaging agent reports myeloperoxidase activity in healing infarcts and noninvasively detects the antiinflammatory effects of atorvastatin on ischemia-reperfusion injury. Circulation. 2008; 117:1153–1160. [PubMed: 18268141]

26. Kim Y, et al. The MEF2D transcription factor mediates stress-dependent cardiac remodeling in mice. J Clin Invest. 2008; 118:124–132. [PubMed: 18079970]

27. Wu CY, Hsieh HL, Sun CC, Yang CM. IL-1beta induces MMP-9 expression via a Ca(2)-dependent CaMKII/JNK/c-JUN cascade in rat brain astrocytes. Glia. 2009

28. Munaut C, et al. Murine matrix metalloproteinase 9 gene. 5'-upstream region contains cis-acting elements for expression in osteoclasts and migrating keratinocytes in transgenic mice. J Biol Chem. 1999; 274:5588–5596. [PubMed: 10026175]

29. Backs J, Song K, Bezprozvannaya S, Chang S, Olson EN. CaM kinase II selectively signals to histone deacetylase 4 during cardiomyocyte hypertrophy. J Clin Invest. 2006; 116:1853–1864. [PubMed: 16767219]

30. Naya FJ, Wu C, Richardson JA, Overbeek P, Olson EN. Transcriptional activity of MEF2 during mouse embryogenesis monitored with a MEF2-dependent transgene. Development. 1999; 126:2045–2052. [PubMed: 10207130]

31. Kolodziejczyk SM, et al. MEF2 is upregulated during cardiac hypertrophy and is required for normal post-natal growth of the myocardium. Current biology : CB. 1999; 9:1203–1206. [PubMed: 10531040]

32. Chang S, et al. Histone deacetylase 7 maintains vascular integrity by repressing matrix metalloproteinase 10. Cell. 2006; 126:321–334. [PubMed: 16873063]

33. Hiratsuka S, et al. MMP9 induction by vascular endothelial growth factor receptor-1 is involved in lung-specific metastasis. Cancer Cell. 2002; 2:289–300. [PubMed: 12398893]

34. Timmins JM, et al. Calcium/calmodulin-dependent protein kinase II links ER stress with Fas and mitochondrial apoptosis pathways. J Clin Invest. 2009; 119:2925–2941. [PubMed: 19741297]

35. Zhao BQ, et al. Role of matrix metalloproteinases in delayed cortical responses after stroke. Nat Med. 2006; 12:441–445. [PubMed: 16565723]

36. Khoo MS, et al. Death, cardiac dysfunction, and arrhythmias are increased by calmodulin kinase II in calcineurin cardiomyopathy. Circulation. 2006; 114:1352–1359. [PubMed: 16982937]

37. Backs J, et al. The delta isoform of CaM kinase II is required for pathological cardiac hypertrophy and remodeling after pressure overload. Proc Natl Acad Sci U S A. 2009; 106:2342–2347. [PubMed: 19179290]

38. Doerries C, et al. Critical role of the NAD(P)H oxidase subunit p47phox for left ventricular remodeling/dysfunction and survival after myocardial infarction. Circ Res. 2007; 100:894–903. [PubMed: 17332431]

39. Kinugawa S, et al. Treatment with dimethylthiourea prevents left ventricular remodeling and failure after experimental myocardial infarction in mice: role of oxidative stress. Circ Res. 2000; 87:392–398. [PubMed: 10969037]

40. Yusuf S, Dagenais G, Pogue J, Bosch J, Sleight P. Vitamin E supplementation and cardiovascular events in high-risk patients. The Heart Outcomes Prevention Evaluation Study Investigators. N Engl J Med. 2000; 342:154–160. [PubMed: 10639540]

41. Rapola JM, et al. Randomised trial of alpha-tocopherol and beta-carotene supplements on incidence of major coronary events in men with previous myocardial infarction. Lancet. 1997; 349:1715–1720. [PubMed: 9193380]

42. MRC/BHF Heart Protection Study of antioxidant vitamin supplementation in 20,536 high-risk individuals: a randomised placebo-controlled trial. Lancet. 2002; 360:23–33. [PubMed: 12114037]

43. Jauslin ML, Meier T, Smith RA, Murphy MP. Mitochondria-targeted antioxidants protect Friedreich Ataxia fibroblasts from endogenous oxidative stress more effectively than untargeted antioxidants. FASEB J. 2003; 17:1972–1974. [PubMed: 12923074]

44. Chen CH, et al. Activation of aldehyde dehydrogenase-2 reduces ischemic damage to the heart. Science. 2008; 321:1493–1495. [PubMed: 18787169]

45. Tomaselli GF, Barth AS. Sudden cardio arrest: oxidative stress irritates the heart. Nat Med. 2010; 16:648–649. [PubMed: 20526319]

46. Maack C, et al. Oxygen free radical release in human failing myocardium is associated with increased activity of rac1-GTPase and represents a target for statin treatment. Circulation. 2003; 108:1567–1574. [PubMed: 12963641]

47. Dargie HJ. Effect of carvedilol on outcome after myocardial infarction in patients with left-ventricular dysfunction: the CAPRICORN randomised trial. Lancet. 2001; 357:1385–1390. [PubMed: 11356434]

48. Dickstein K, Kjekshus J, Group, O.S.C.o.t.O.S. Effects of losartan and captopril on mortality and morbidity in high-risk patients after acute myocardial infarction: the OPTIMAAL randomised trial. Optimal Trial in Myocardial Infarction with Angiotensin II Antagonist Losartan. Lancet. 2002; 360:752–760. [PubMed: 12241832]

49. Christensen MD, et al. Oxidized calmodulin kinase II regulates conduction following myocardial infarction: a computational analysis. PLoS Comput Biol. 2009; 5:e1000583. [PubMed: 19997488]

50. Wehrens XH, Doevendans PA. Cardiac rupture complicating myocardial infarction. Int J Cardiol. 2004; 95:285–292. [PubMed: 15193834]

51. Pouleur AC, et al. Pathogenesis of sudden unexpected death in a clinical trial of patients with myocardial infarction and left ventricular dysfunction, heart failure, or both. Circulation. 2010; 122:597–602. [PubMed: 20660803]

52. Fonarow GC, Lukas MA, Robertson M, Colucci WS, Dargie HJ. Effects of carvedilol early after myocardial infarction: analysis of the first 30 days in Carvedilol Post-Infarct Survival Control in Left Ventricular Dysfunction (CAPRICORN). Am Heart J. 2007; 154:637–644. [PubMed: 17892984]

53. Ambrosioni E, Borghi C, Magnani B. The effect of the angiotensin-converting-enzyme inhibitor zofenopril on mortality and morbidity after anterior myocardial infarction. The Survival of Myocardial Infarction Long-Term Evaluation (SMILE) Study Investigators. N Engl J Med. 1995; 332:80–85. [PubMed: 7990904]

54. Beygui F, et al. Rationale for an early aldosterone blockade in acute myocardial infarction and design of the ALBATROSS trial. Am Heart J. 2010; 160:642–648. [PubMed: 20934557]

55. Weiss RM, Ohashi M, Miller JD, Young SG, Heistad DD. Calcific aortic valve stenosis in old hypercholesterolemic mice. Circulation. 2006; 114:2065–2069. [PubMed: 17075015]

56. Thiel WH, et al. Proarrhythmic defects in Timothy syndrome require calmodulin kinase II. Circulation. 2008; 118:2225–2234. [PubMed: 19001023]

57. Mohler PJ, et al. Defining the cellular phenotype of "ankyrin-B syndrome" variants: human ANK2 variants associated with clinical phenotypes display a spectrum of activities in cardiomyocytes. Circulation. 2007; 115:432–441. [PubMed: 17242276]

58. Li H, et al. Calmodulin kinase II is required for angiotensin II-mediated vascular smooth muscle hypertrophy. Am J Physiol Heart Circ Physiol. 2010; 298:H688–698. [PubMed: 20023119]

59. Brot N, Weissbach L, Werth J, Weissbach H. Enzymatic reduction of protein-bound methionine sulfoxide. Proc Natl Acad Sci U S A. 1981; 78:2155–2158. [PubMed: 7017726]

60. Owusu-Ansah E, Yavari A, Banerjee U. A protocol for in vivo detection of Reactive Oxygen Species. Y1 - 2008 Y2 - 3 February. - *Nature protocols M1 - Journal Article*. 2008
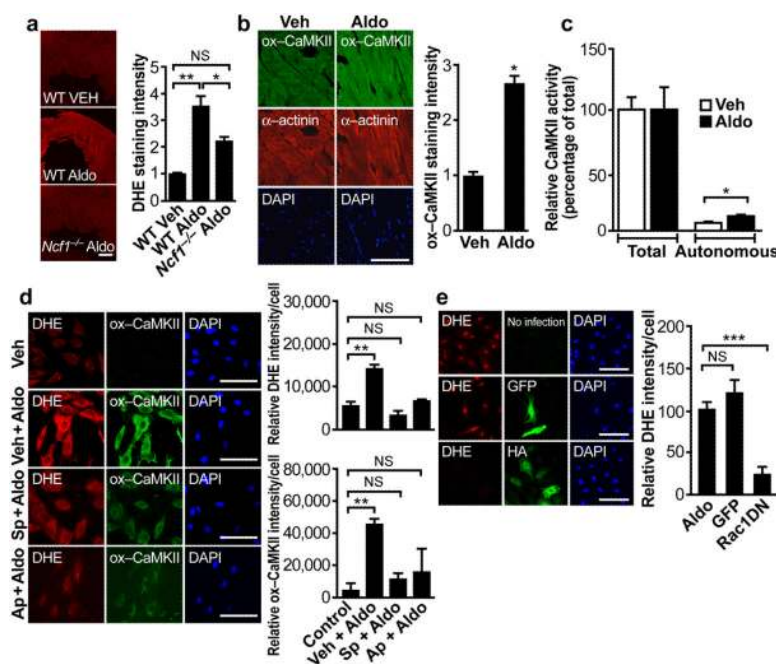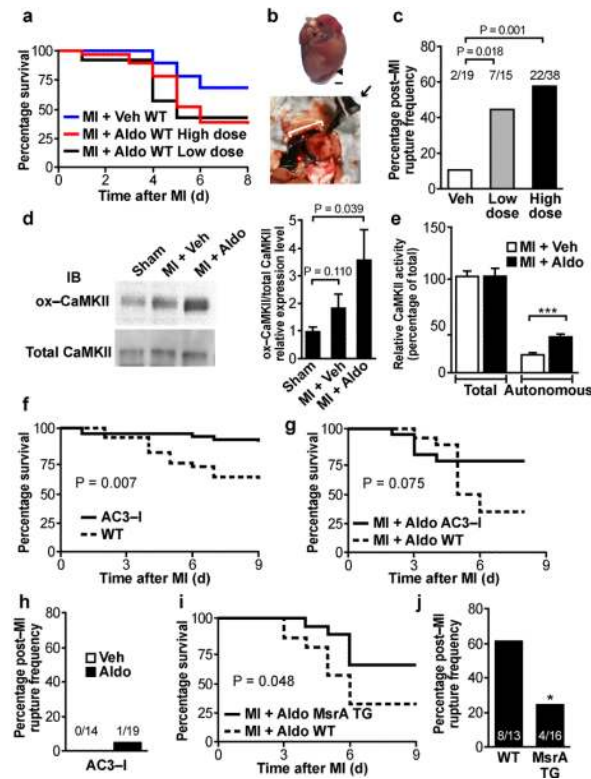
Figure 1.
ROS and CaMKII oxidation and activation by Aldo. **(a)** Representative images of DHE fluorescence in viable, cryopreserved myocardium after 15 minutes Aldo (10^{-7} mol L^{-1}) stimulation in $Ncf1^{-/-}$ and WT mice. Scale bar = 0.5 mm. Summary data, $P = 0.003$, One-way ANOVA, $*P < 0.05$ and $**P < 0.01$ Bonferroni's multiple comparison test. $n \geq 3$ mice per genotype. **(b)** Representative immunofluorescence images after chronic Aldo infusion (1.44 mg kg^{-1} d^{-1}, 2 weeks) showing enhanced CaMKII oxidation (ox-CaMKII, green) in left ventricular sections. α-actinin (red) marks myocardium. DAPI (blue) marks nuclei. Scale bar = 100 μm. $*P = 0.008$. $n \geq 3$ mice per treatment. **(c)** Autonomous, Ca^{2+}/calmodulin-independent and total, Ca^{2+}/calmodulin-dependent CaMKII activity after Aldo and Veh infusion. $*P = 0.019$, Student's t-test. $n \geq 5$ mice per treatment. **(d)** Aldo treatment for 15 minutes (10^{-7} mol L^{-1}) increased DHE fluorescence and ox-CaMKII more than Veh-treated WT neonatal myocytes. Pretreatment with spironolactone (Sp, MR antagonist, 10^{-1} μmol L^{-1}) or apocynin (Ap, NADPH oxidase inhibitor, 100 μmol L^{-1}) reduces Aldo-induced DHE and ox-CaMKII. Summary data for both DHE intensity and ox-CaMKII, $P < 0.001$, One-way ANOVA, $***P < 0.001$ Bonferroni's multiple comparison test versus Control. Scale bar = 100 μm. **(e)** Expression of an HA tagged dominant negative Rac1 mutant (HA) prevented Aldo stimulated increases in DHE fluorescence. $P < 0.001$, One-way ANOVA, $***P < 0.001$ Bonferroni's multiple comparison test versus Aldo. Scale bar = 100 μm.
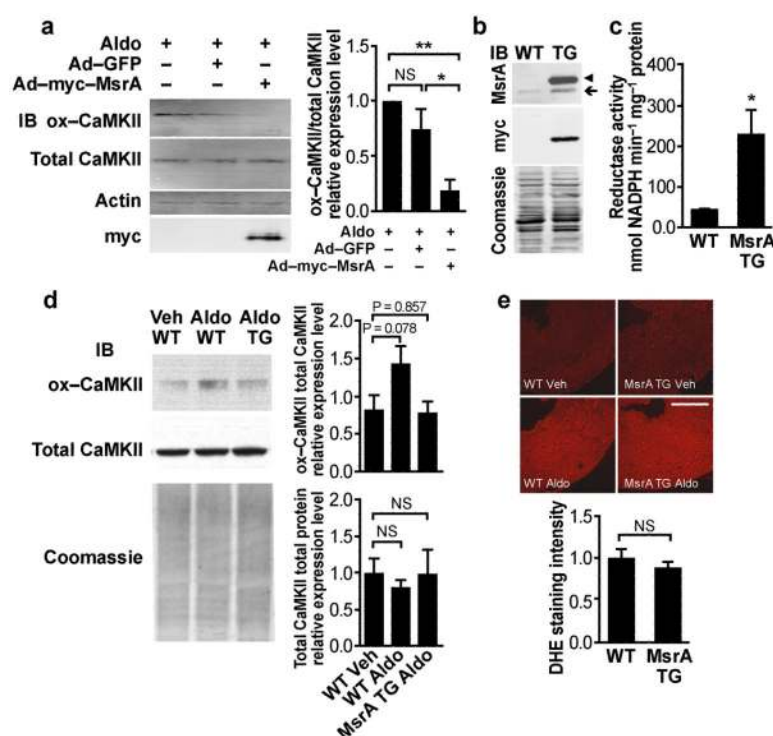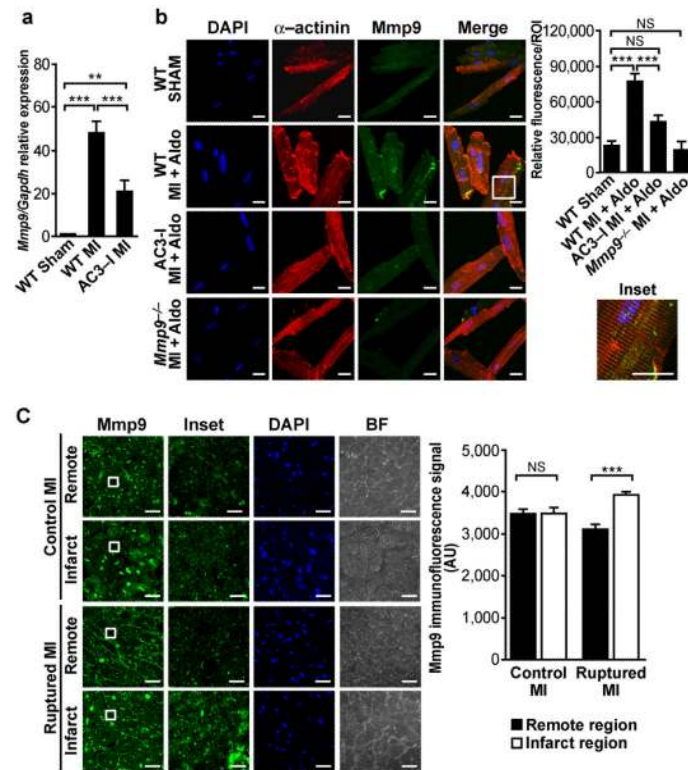
Figure 2.
Transgenic (TG) myocardial MsrA over-expression reduces CaMKII oxidation. **(a)**
Representative immunoblot of CaMKII oxidation in neonatal myocytes. CaMKII oxidation
is reduced by pre-infection with an adenoviral construct over-expressing myc tagged human
MsrA. Summary data for $n = 3$ trials, $P = 0.008$, One-way ANOVA, $*P < 0.05$, $**P < 0.01$,
Bonferroni's multiple comparison test versus Aldo-treated, non-infected control. **(b)**
Representative immunoblot shows over-expression of MsrA in hearts from transgenic mice.
The myc tagged human MsrA transgene (◄) runs higher than endogenous MsrA (←). **(c)**
Cardiac MsrA activity is increased in transgenic mice compared to WT littermates. $*P =$
0.035, Student's t-test, $n \geq 3$ mice per genotype. **(d)** WT mice infused with Aldo (1.44 mg
kg^{-1} d^{-1}, 2 weeks) show a substantial trend towards increased CaMKII oxidation by
Western blotting in total heart homogenates, $P = 0.078$. MsrA transgenic mice appear
resistant to Aldo-induced CaMKII oxidation. Total cardiac CaMKII expression levels
remain similar between MsrA transgenic mice and WT control littermates, $n = 6$ mice per
genotype. **(e)** DHE fluorescence of viable, cryopreserved myocardium after 15 minutes Aldo
(10^{-7} mol L^{-1}) stimulation. Aldo increases DHE fluorescence similarly in MsrA transgenic
and WT hearts. Scale bar = 1 mm. $n \geq 3$ mice per genotype.

Figure 3.
Aldo increases mortality after MI by promoting myocardial rupture. **(a)** Kaplan-Meier survival curve for WT mice after MI + Veh versus MI + Aldo. $n \geq 15$ mice per treatment. **(b)** Necropsy of a representative MI + Aldo WT mouse. Forceps (→) retracts clotted blood from ruptured heart. Rupture site (◄). Scale bar = 1 mm. **(c)** Rupture frequency in WT mice after MI + Aldo, at Low dose and High dose (see Supplemental Fig. 4 and Methods), Chi-square test, $P = 0.018$ and $P = 0.001$, respectively. **(d)** Representative immunoblot from post-MI cardiac lysates for ox-CaMKII two weeks after surgery. Summary data for $n = 6$ mice per treatment. **(e)** Autonomous and total CaMKII activity in WT MI + Aldo versus MI + Veh mice. ***$P < 0.001$, Student's t-test, $n \geq 5$ mice per treatment. **(f)** Kaplan-Meier survival curve for WT littermate and AC3-I mice after MI, $n \geq 30$ mice per genotype, $P = 0.007$. **(g)** Kaplan-Meier survival curve for AC3-I and WT mice after MI + Aldo. $n = 15–19$ mice per genotype, $P = 0.075$. **(h)** Summary data showing rupture protection in AC3-I mice after MI + Aldo or MI + Veh. **(i)** Kaplan-Meier survival curve for WT littermate and MsrA transgenic (TG) mice after MI + Aldo. $n = 13–16$ mice per genotype, $P = 0.048$. **(j)** Rupture frequency in WT littermate and MsrA TG mice after MI + Aldo. $n = 13–16$ mice per genotype, *$P = 0.047$.
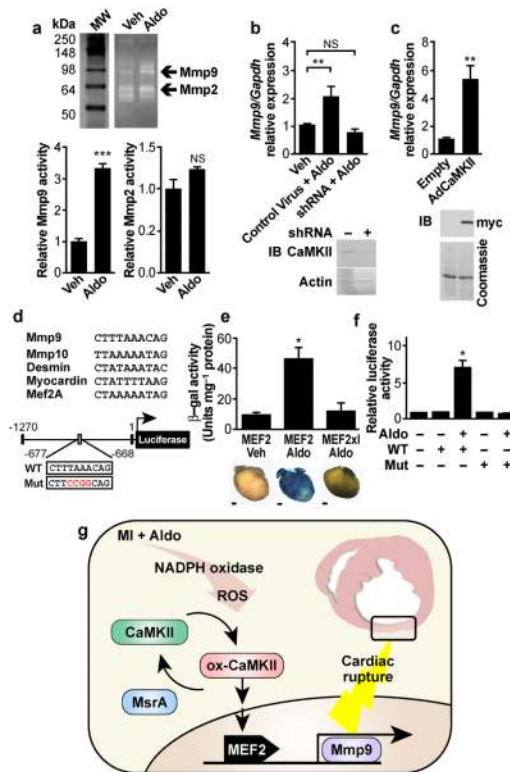
Figure 4.
Mmp9 levels in mouse and human hearts. **(a)** Relative *Mmp9* mRNA levels 3 days post-MI in WT and AC3-I mice. $P < 0.0001$, One-way ANOVA, $n \geq 3$ mice per treatment, **$P < 0.01$, ***$P < 0.001$, Bonferroni's multiple comparison test. **(b)** Immunofluorescence of isolated adult mouse ventricular myocytes 24 hours after MI shows increased Mmp9 expression in MI + Aldo compared to Sham operated controls and to $Mmp9^{-/-}$ controls. Myocytes from AC3-I mice have lower Mmp9 expression compared to WT myocytes. All images are maximum projections from z-stacks obtained by confocal microscopy. Inset shows Mmp9 expression is cytoplasmic and appears perpendicular to α-actinin staining. Scale bar = 20 μm. Quantification of immunofluorescence. $P < 0.0001$, One-way ANOVA, ***$P < 0.001$, Bonferroni's multiple comparison test. At least 10 regions of interest were selected from $n = 5$–10 cells per treatment. **(c)** Immunofluorescence for Mmp9 in human myocardium from MI subjects without rupture (Control MI) and with rupture (Ruptured MI). Images are the maximum projection of z-stacks acquired with confocal microscopy. Brightfield (BF) images show cross-sectional myocardial cells in bundles. Inset shows intracellular staining of Mmp9. Quantification of intracellular regions of interest were confined to cardiomyocytes and show an increased speckled and punctate staining pattern for Mmp9 within cardiomyocytes from humans with ruptured MI and no gradient in Mmp9 signal in control MI samples, $P < 0.001$, One-way ANOVA, $n \geq 5$ specimens per group, ***$P < 0.001$, Bonferroni's multiple comparison test. Scale bar = 25 μm.
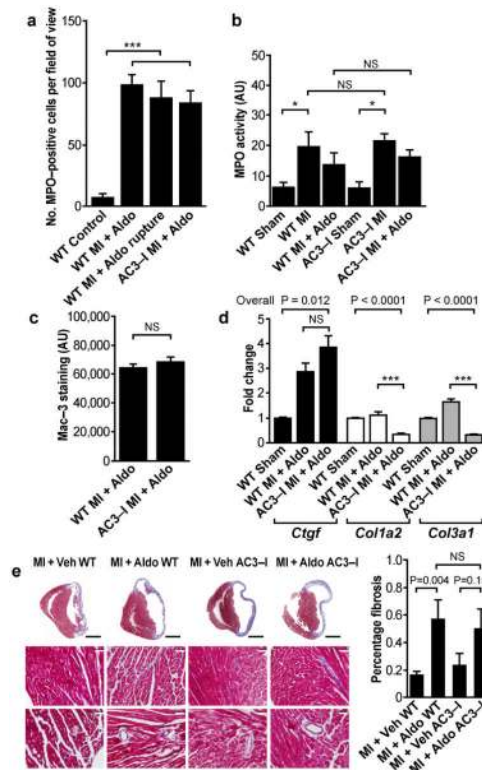
Figure 5.
Characterization of inflammatory and fibrotic response between AC3-I and WT mice after MI + Aldo. **(a)** The number of MPO positive cells identified on immunohistochemistry of heart tissue sections is similar between WT and AC3-I mice 24 hours after MI + Aldo and between ruptured and non-ruptured WT MI + Aldo mice. $P < 0.001$, One-way ANOVA, $n \geq$ 3 mice per group, ***$P < 0.001$, Bonferroni's multiple comparison test. **(b)** MPO activity is similar between WT and AC3-I mice. MPO activity increases after MI in both WT and AC3-I mice. AC3-I mice show no difference to WT mice even after MI + Aldo. $P = 0.001$, One-way ANOVA, $n \geq 3$ mice per group, *$P < 0.05$, Bonferroni's multiple comparison test. **(c)** Cumulative Mac-3 staining is similar in AC3-I mice compared to WT mice 3 days after MI + Aldo. $n \geq 3$ mice per group. **(d)** Differential regulation of pro-fibrotic genes after MI + Aldo in WT and AC3-I mice, *Ctgf* = connective tissue growth factor, *Col1a2* = collagen type I alpha 2, *Col3a1* = collagen type III alpha 1, $n \geq 4$ mice per group, One-way ANOVA, ***$P < 0.001$, Bonferroni's multiple comparison test. **(e)** Masson's trichrome staining shows similar increase in fibrosis after MI + Aldo in both WT and AC3-I. Student's t-test versus MI + Veh, $n \geq 3$ mice per group. Black scale bar = 2 mm. White scale bar = 50 μm.

Figure 6.
CaMKII promotes cardiac Mmp9 expression and activity. **(a)** Representative gelatin zymogram for Mmp9 and Mmp2 activity in culture supernatant bathing neonatal myocytes, ***P < 0.001, n = 4 assays per treatment. **(b)** qRT-PCR for *Mmp9* in total RNA isolated from neonatal myocytes after 24 hour Aldo treatment with or without CaMKII knockdown by shRNA. Overall P < 0.001, One-way ANOVA, **P < 0.01 Bonferroni's multiple comparison test. Immunoblot verifies CaMKII knockdown. **(c)** CaMKII over-expression increases *Mmp9* mRNA expression compared to control empty virus, **P = 0.002. Immunoblot verifies over-expression of myc-tagged CaMKII. **(d)** Alignment of the putative MEF2 binding domain from mouse Mmp9 promoter with bona fide MEF2 binding domains. Schematics of *Mmp9* promoter luciferase reporter constructs: WT and control (Mut). **(e)** β-galactosidase expression and activity after Aldo infusion in MEF2-lacZ reporter mice and MEF2-lacZ reporter mice interbred with AC3-I mice (MEF2xI). Scale bar = 1 mm. n ≥ 3 mice per group, P = 0.002, One-way ANOVA, *P < 0.05 Bonferroni's multiple comparison test versus Veh. **(f)** *Mmp9* promoter driven luciferase activity after Aldo treatment, comparing WT and mutant constructs, normalized to cotransfected *Renilla* luciferase plasmid. P < 0.001, One-way ANOVA, *P < 0.05 Bonferroni's multiple comparison test versus control. **(h)** Proposed model for MI + Aldo-induced CaMKII activation leading to myocardial rupture. In the acute post-MI setting, ox-CaMKII leads to Mmp9 upregulation to accelerate matrix breakdown, leading to cardiac rupture and premature death. MsrA reduces ox-CaMKII to prevent Mmp9 expression and protect against post-MI cardiac rupture.